RESEARCH ARTICLE

Radionuclides in the soil around the largest coal-fired power plant in Serbia: radiological hazard, relationship with soil characteristics and spatial distribution

Mirjana Ćujić · Snežana Dragović · Milan Đorđević ·
Ranko Dragović · Boško Gajić · Šćepan Miljanić

Abstract Primordial radionuclides, ^{238}U, ^{232}Th and ^{40}K were determined in soil samples collected at two depths (0–10 and 10–20 cm) in the vicinity of the largest coal-fired power plant in Serbia, and their spatial distribution was analysed using ordinary kriging. Mean values of activity concentrations for these depths were 50.7 Bq kg^{-1} for ^{238}U, 48.7 Bq kg^{-1} for ^{232}Th and 560 Bq kg^{-1} for ^{40}K. Based on the measured activity concentrations, the radiological hazard due to naturally occurring radionuclides in soil was assessed. The value of the mean total absorbed dose rate was 76.3 nGy h^{-1}, which is higher than the world average. The annual effective dose due to these radionuclides ranged from 51.4 to 114.2 μSv. Applying cluster analysis, correlations between radionuclides and soil properties were determined. The distribution pattern of natural radionuclides in the environment surrounding the coal-fired power plant and their enrichment in soil at some sampling sites were in accordance with dispersion models of fly ash emissions. From the results obtained, it can be concluded that operation of the coal-fired power plant has no significant negative impact on the surrounding environment with regard to the content of natural radionuclides.

Abbreviations

CC	carbonate content
CEC	Cation exchange capacity
CF	Contamination factor
CA	Cluster analysis
SEC	Specific electrical conductivity
CFPP	Coal-fired power plant
TOC	Total organic carbon

M. Ćujić (✉)
University of Belgrade—Institute for the Application of Nuclear Energy, Banatska 31b, 11080 Belgrade, Serbia
e-mail: cujicm@inep.co.rs

S. Dragović
University of Belgrade—Vinča Institute of Nuclear Sciences, PO Box 522, 11001 Belgrade, Serbia

M. Đorđević · R. Dragović
Department of Geography, University of Niš—Faculty of Science and Mathematics, Višegradska 33, 18000 Niš, Serbia

B. Gajić
Institute of Land Management, University of Belgrade—Faculty of Agriculture, Nemanjina 6, 11081 Belgrade, Serbia

Š. Miljanić
University of Belgrade—Faculty of Physical Chemistry, Studentski trg 12-16, Belgrade 11158, Serbia

Introduction

Natural environmental radioactivity and the associated external exposure to gamma radiation depend primarily on geological and geographical conditions and appear at different levels in the soils of each region in the world (UNSCEAR 2010). Knowledge of natural radionuclide distribution in soils is important for assessing radiation exposure to the population and is useful to set standards and national guidelines in accordance with international recommendations. Radiation risk from natural radioactivity enhanced by human activity exists in many branches of the non-nuclear industry, where raw materials, products and remains could contain enhanced concentrations of radionuclides. It is necessary to study radiation and radioactivity in order to have reference data for documenting changes in environmental radioactivity in soil

due to human activities. Millions of tons of coal are burnt every year in coal-fired power plants (CFPPs) worldwide, producing naturally occurring radioactive material waste, generated at each step of the process, starting from mining the ore through transportation and combustion in a power plant and deposition of ash in sludge lagoons. The physical and chemical composition of coal combustion residues varies considerably, depending on the quality of the feed coal, the combustion technology, the fraction considered and the method of disposal. Dumping fly ash may increase the radiation level around the dump site. In addition to meteorological conditions, the distance that particles travel depends on particle size and stack height (Clarke and Sloss 1992; Papastefanou 2010). Populations living in the vicinity of CFPPs are exposed more or less to enhanced levels of natural radionuclides, and the main pathways are inhalation, external irradiation and ingestion following deposition on the ground. According to UNSCEAR (2010), the world average activity concentrations for ^{238}U, ^{232}Th and ^{40}K in soils are 33, 45 and 412 Bq kg^{-1}, respectively. Based on the reported results, average mean activity concentrations of ^{238}U, ^{232}Th and ^{40}K in soils of Serbia were 43.1, 45.3 and 500 Bq kg^{-1}, respectively (Bikit et al. 2005; Dragović and Onjia 2006; Janković-Mandić et al. 2010). In recent years, a number of studies have dealt with the impact of environmental radioactivity from CFPPs (Aytekin and Baldik 2008; Charro et al. 2013a; Dai et al. 2007; Lu et al. 2012; Papp et al. 2002; Parmaksiz et al. 2011). Different multivariate chemometric tools have been applied to identify the most important factors explaining the variability in environmental data, including radionuclide activity concentrations (Bhuiyana et al. 2010; Charro et al. 2013b; Dragović and Onjia 2006; Külahci and Şen 2008; Tsikritzis 2005).

The aims of this study were as follows: (i) to determine the content of radionuclides (^{238}U, ^{232}Th and ^{40}K) in soil samples in the vicinity of the largest CFPP in Serbia, (ii) to estimate the dose rate and hazard index of gamma-ray radiation for the population, (iii) to investigate hierarchical correlations between radionuclides in soil and soil properties and (iv) to use ordinary kriging to analyse the spatial distribution of the determined radionuclides.

Materials and methods

Study area and sampling

The CFPP complex 'Nikola Tesla' consisting of two blocks (*A* and *B*) are situated in western Serbia in the municipality of Obrenovac (N 44° 39′, E 20° 11′), on the right bank of the river Sava, 42 km upstream from Belgrade, the Serbian capital city. There are around 75,000 people living in the municipality of Obrenovac. The CFPP 'Nikola Tesla' complex contains eight units with total installed capacity of 2892 MW and uses

lignite from the Kolubara open coal mine. Annual production of coal ash is three to four million tons. The ash disposal sites of CFPP 'Nikola Tesla' cover an area of 900 ha. Coal ash is stored at the dump after being suspended in water taken from the river Sava. Ilic et al. (2003) reported that fly ashes derived during combustion of lignite in CFPP 'Nikola Tesla' belong to class C according to ASTM C 618-92 classification (ASTM 1988).

Samples of undisturbed soils that had not been cultivated were taken during 2011 from 72 locations (Fig. 1) applying the 'systematic random sampling' procedure (IAEA 2004). Samples were taken at depths of 0–10 cm (A) and 10–20 cm (B), and the locations were recorded using an eTrex Vista Garmin handheld Global Positioning System (GPS) with precision of ±10 m (IAEA 2004; ASTM C 998-83 1983). Soil samples were collected with a stainless steel spade and packed immediately in plastic bags. To avoid cross contamination, the equipment was first brushed to eliminate residues from the previous specimen and then flushed with soil from the new sampling site. After drying to constant weight at room temperature in the laboratory, the soil samples were homogenized and passed through a 2-mm sieve.

Geological and pedologic settings of the study area

Devonian–Carboniferous, Medium and Upper Permian, Lower and Middle Triassic, Jurassic, Lower and Upper Cretaceous, Neogene and Quaternary sediments are arranged superpositionally in the investigated area (Federal Geological Survey 1980). The wider Kolubara basin was affected by volcanic activity during the Middle Miocene. Coals from the Kolubara basin were formed during the Upper Miocene in a limnic clastic depositional environment (Životić et al. 2008). The diameter of the basin bottom is more than 30 km, and the greatest height in the eastern and southern parts ranges between 370 and 390 m. The altitude of the area decreases from the east to central parts of the basin (120–160 m) and from the southern edge (Tamnava) to the alluvial plain of the river Sava.

Most of the studied area consists of alluvial soil (Calcaric Fluvisols) with loamy-clay characteristics (Institute of Soil Science 1963). Gleysols are represented in fragments of the west meander neck. To the south, the Gleysols continue as Humic Gleysols, of 1.5-km average width and about 4 km in length in the west–east direction. The Eutric Cambisols are continuous, while the Calcaric Fluvisols extend from the confluence of the Kolubara and Tamnava to the south and cover the area around the upper course of the river Kolubara and Peštan (Poljane). In the area of Obrenovac, the anthropogenic soils (Technosols) also occurred, as a result of operation of CFPPs. Technogenic soils are present in a relatively small area, but in some locations across them, alohtone natural soils are deposited. These are ash and flotation material (Spolic Regosols) near Obrenovac power plants and in Veliki

Fig. 1 Simplified pedologic map of the study area and distribution of sampling sites (the wind frequency increase is presented in the *upper left corner*)
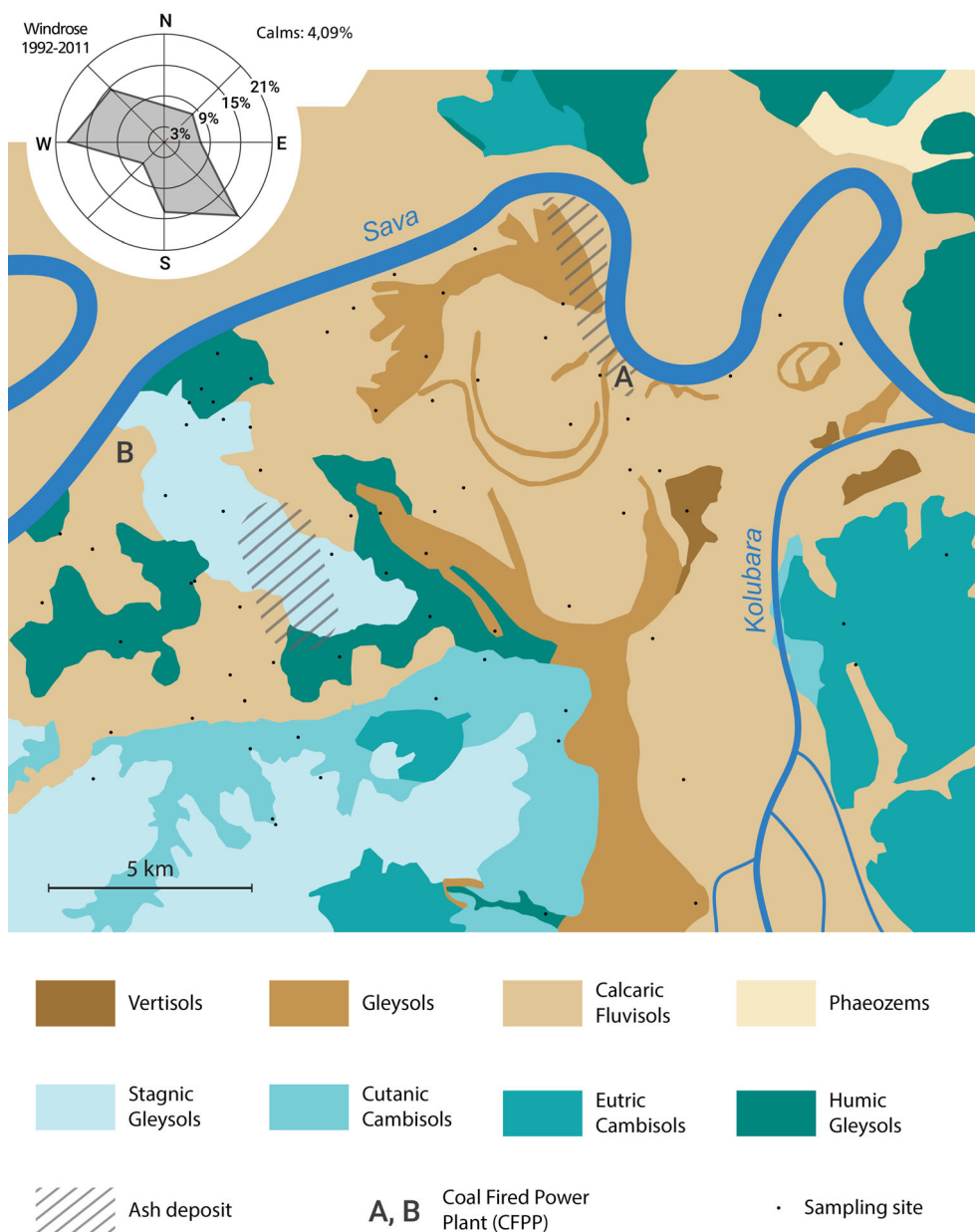
Crljeni. A compact zone of planosol is spread over the area of Dubrava, south-west of Obrenovac. This zone is located between Cutanic Cambisols and Eutric Cambisols and tapers towards the north-east (Fig. 1).

Radioactivity measurements

The activity concentration (Bq kg^{-1}) was determined using a p-type high-purity germanium detector (ORTEC-AMATEC). The resolution and relative efficiency of the detector for 1332 keV (^{60}Co) are 1.65 keV and 35 %, respectively. For energy and efficiency calibration of the detector a mixed calibration source (MBSS 2 type from the Czech Metrological Institute) was used composed of ^{241}Am, ^{109}Cd,

^{139}Ce, ^{57}Co, ^{60}Co, ^{137}Cs, ^{113}Sn, ^{85}Sr, ^{88}Y and ^{203}Hg dispersed in silica resin placed in the Marinelli beaker. Standard reference materials from the IAEA were used for quality assurance and quality control (RGU-1 and RGTh-1). For gamma spectrometry measurements, air-dried, crushed and sieved samples were weighed and placed in Marinelli beakers and hermetically sealed for at least 4 weeks to ensure that radioactive equilibrium was reached between ^{226}Ra, ^{222}Rn and their short-lived daughters. The samples were counted for 60 ks to obtain a spectrum. The activity concentration was determined by measuring the gamma-ray lines at 63.3, 92.35 and 92.78 keV for ^{238}U; 338.4, 911.1 and 968.9 keV for ^{232}Th and 1460.8 keV for ^{40}K. Gamma-ray spectra were analysed using Gamma Vision 32 MCA emulation software (ORTEC

2001). The lower limit of detection for radionuclides of interest was derived from the background measurement of 60 ks and found to be 0.8 Bq kg^{-1} for ^{238}U, 0.4 Bq kg^{-1} for ^{232}Th and 2.1 Bq kg^{-1} for ^{40}K.

Determination of soil properties

The traditional pipette method was used for particle size analysis (Rowell 1997, Soil Conservation Service 1972). Organic matter was removed from the weighed sample with hydrogen peroxide and the remaining mineral particles weighed and subjected to particle size analysis to determine the following fractions: sand (0.05–2 mm), silt (0.002–0.05 mm) and clay (<0.002 mm). Soil pH and specific electrical conductivity were measured in 1:5 soil-water suspensions using a WTW inoLab ph/Cond 720 instrument (ISO 10309 2005; ISO 11265 1994). The total organic carbon content was determined by a titration method, using $(NH_4)_2Fe(SO_4)_2 \times 6H_2O$ after digestion of samples with dichromate-sulphuric acid solution, based on the Tyurin method (Simakov 1957; Walkley and Black 1934). Carbonates were measured volumetrically using Scheibler's calcimeter for $CaCO_3$ content (ISO 10693 1995). The total cation exchange capacity of the sorptive complex was calculated as the sum of the hydrolytic acidity and total exchange bases, both measured according to Baize (1993).

Estimation of dose rate and hazard index of γ-ray radiation

The total absorbed dose rate in air is a relevant quantity when considering radiation risk to humans and other biota. It is calculated using conversion factors to transform the measured activity concentrations A_U, A_{Th}, and A_K (Bq kg^{-1}) of U, Th and K into absorbed dose rate (D) (nGy h^{-1}) (Eq. 1) at 1 m above the ground (UNSCEAR 2000):

$$D = 0.462A_U + 0.604A_{Th} + 0.042A_K \tag{1}$$

The annual effective dose (H) (μSv) (Eq. 2) can be calculated multiplying the estimated absorbed dose rate by factors, where 0.7 Sv Gy^{-1} represents the quotient of annual effective dose received by adults to absorbed dose rate in air, 0.2 is the outdoor occupancy factor and 8760 is the number of hours in 1 year.

$$H = D \times 0.7 \times 0.2 \times 8760 \tag{2}$$

The external hazard index (H_{ex}) (Eq. 3), as defined by Beretka and Mathew (1985), must be less than unity in order to keep the radiation hazard insignificant. The external hazard index is obtained from the radium equivalent activity of 370 Bq kg^{-1} and corresponds to a dose limit of 1.0 mSv for the general population.

$$H_{ex} = \frac{A_U}{370} + \frac{A_{Th}}{259} + \frac{A_K}{4810} \tag{3}$$

Excess lifetime cancer risk outdoors ($ELCR_{outdoor}$) was calculated according to the following equation:

$$ELCR_{outdoor} = H \times LS \times PC \tag{4}$$

where LS—lifespan (average 70 years) and PC—the nominal probability coefficient for detriment-adjusted cancer risk of 0.055 Sv^{-1} for the public (ICRP 2007). This risk represents the number of extra cancers expected in a given number of people exposed to a carcinogen at a given dose.

Statistical analysis

Cluster analysis (CA) was used in this study to distinguish correlations between radionuclides and soil properties. The aim of CA is to optimize the heterogeneity between groups as well as the homogeneity within them. The cluster method defines the rules for cluster formation. Correlation between two objects reflects the degree to which they are related. The Pearson product moment correlation coefficient was used as the measure of correlation. Calculation in CA moves forwards in an agglomerative way until all objects are joined in a single cluster. Usually, the results are presented as a dendrogram, in which the distance within clusters represents the degree of association between the elements. Details on CA can be found in standard chemometric textbooks (Brereton 2003). The Statistical Package for the Social Sciences (SPSS 16.0) was used for descriptive statistics of data and CA (SPSS 2007).

Geostatistical data were modelled using ArcGIS mapping software (ESRI 2009) by the Geostatistical Analyst extension. The kriging method was chosen because it has advantages over other interpolation techniques. Among kriging procedures, the ordinary kriging method is most commonly used for environmental situations.

Geostatistics is based on the theory of a regionalized variable (Matheron 1963), which shows spatial autocorrelation where observations close to each other are more alike than those that are far apart. Semivariogram function is defined as half the averaged squared difference between paired data values separated by a distance interval (Matheron 1965).

$$\gamma(h) = \frac{1}{2H(h)} \sum_{i=1}^{N(h)} \{Z(X_i) - Z(X_i + h)\}^2 \tag{5}$$

where $\gamma(h)$ is the semivariogram, $N(h)$ the number of pairs of sample points, $Z(X_i)$ is the radionuclide concentration value measured at location X_i, h is the distance between sample points and X_i is the sample position.

Cross validation was used to compare the measured and predicted values for each radionuclide concentration. Four types of semivariogram models (circular, spherical, exponential and Gaussian) were tested. To find out which model is best at predicting values, the mean error (ME), root-mean-square error (RMSE), average standard error (ASE), mean square error (MSE) and root-mean-square standardized error (RMSSE) were calculated. Because kriging is unbiased, the ME should be near zero. MSE was used to standardize the mean error, which ideally should also be zero. The RMSE and average standard error should be as close as possible. If the predictions are close to the measured values, the RMSSE should be close to 1. If the RMSSE is greater than 1, the predicted values are underestimated, and if the RMSSE is less than 1, the predicted values are overestimated. Also, the RMSE should be small (Dai et al. 2007).

$$ME = \frac{1}{N} \sum_{i=1}^{N} \left\{ Z(X_i) - \widehat{Z}(X_i) \right\}^2 \tag{6}$$

$$RMSE = \sqrt{\frac{1}{N} \sum_{i=1}^{N} \left\{ Z(X_i) - \widehat{Z}(X_i) \right\}^2} \tag{7}$$

$$ASE = \sqrt{\frac{1}{N} \sum_{i=1}^{N} \sigma^2(X_i)} \tag{8}$$

$$RMSE = \sqrt{\frac{1}{N} \sum_{i=1}^{N} \left(\frac{ME}{\sigma^2(X_i)} \right)^2} \tag{9}$$

$$MSE = \frac{1}{N} \sum_{i=1}^{N} \frac{ME}{\sigma^2(X_i)} \tag{10}$$

where N is number of values in the dataset, $Z(X_i)$ is the measured value, (X_i) is the predicted value and σ^2 is the kriging variance for location X_i.

Results and discussion

Primordial radionuclides in soil and soil properties

Descriptive statistics of radionuclides and soil properties in soil samples from 72 locations around CFPP 'Nikola Tesla' in depth A (0–10 cm), B (10–20 cm) and the average for both depths are summarized in Table 1. Within depth A, the activity concentration range for ^{238}U was 31–67 Bq kg^{-1}, for ^{232}Th 25–60 Bq kg^{-1}, and for ^{40}K, it was 345–733 Bq kg^{-1}. Within depth B, the activity concentration range for ^{238}U was 21–82 Bq kg^{-1}, for ^{232}Th 15–61 Bq kg^{-1} and for ^{40}K 275–751 Bq kg^{-1}. The highest concentrations of ^{40}K were found at locations close to the CFPP, and the highest amounts of ^{238}U and ^{232}Th occurred to the south and west of the power plant, which coincided with the results obtained from dispersion models of fly ash emissions in the study area (Milutinović et al. 2012). Normal distribution of measured data is desirable, but when this is not the case, transformations can make the values more normally distributed (Gokalp et al. 2010). Some of the datasets did not show normal distribution, so logarithmic and Box–Cox transformations were performed. The Box–Cox transformations

Table 1 Descriptive statistics of activity concentration (Bq kg^{-1}) of radionuclides for depths A and B and for the average for both depths in soil samples and estimated D (nGy h^{-1}), H (μSv), H_{ex} and ELCR around CFPP 'Nikola Tesla'

Parameter	^{238}U			^{232}Th			^{40}K			D	H	H_{ex}	ELCR$\times 10^{-4}$
Depth	A	B	Both	A	B	Both	A	B	Both				
Descriptive statistics													
Mean	50.8	50.6	50.7	48.3	48.8	48.6	557	564	560	76.3	93.6	0.4	3.6
Range	36	61	44	35	46	38	388	476	367	51.1	62.7	0.3	2.4
Standard deviation	10.3	12.6	10.4	8.5	9.1	8.6	88.4	88.4	85.2	11.2	13.7	0.06	0.5
Minimum	31.3	20.5	25.9	25.1	14.9	23.4	344.8	275.3	374.6	41.9	51.4	0.24	2.0
Maximum	66.7	81.7	74.2	60.3	60.8	60.6	732.6	751.2	741.9	93.1	114.1	0.54	4.4

decreased skewness and kurtosis, so they were applied in further work except for ^{40}K data from depth A with skewness 0.001 and kurtosis 2.158. After Box–Cox transformation, ^{238}U and ^{232}Th skewness values in depth A were 0.004 and −0.008 and in depth B 0.015 and 0.008, respectively, while that for ^{40}K was 0.021. Kurtosis values for ^{238}U and ^{232}Th were 1.876 and 1.840 in depth A and 2.689 and 2.088, respectively, in

depth B, while that for K was 2.991. Histograms and QQ plots of normalized data for all three radionuclides are presented in Fig. 2. Non-normal distribution of ^{238}U and ^{232}Th could be attributed to their anthropogenic origin, while non-normal distribution of ^{40}K might be due to root uptake of this element in depth B.

In the vicinity of CFPP block *A* at the depth of 6 m, activity concentrations of ^{238}U, ^{232}Th and ^{40}K in soil

Fig. 2 The histograms and probability plots of ^{238}U, ^{232}Th and ^{40}K concentrations in soils from the study area

Histogram of ^{238}U concentrations (Bq kg^{-1}) - depth A

Normal QQ plot of ^{238}U concentrations - depth A

Histogram of ^{238}U concentrations (Bq kg^{-1}) - depth B

Normal QQ plot of ^{238}U concentrations - depth B

Histogram of ^{232}Th concentrations (Bq kg^{-1}) - depth A

Normal QQ plot of ^{232}Th concentrations - depth A

Histogram of ^{232}Th concentrations (Bq kg^{-1}) - depth B

Normal QQ plot of ^{232}Th concentrations - depth B

Histogram of ^{40}K concentrations (Bq kg^{-1}) - depth A

Normal QQ plot of ^{40}K concentrations - depth A

Histogram of ^{40}K concentrations (Bq kg^{-1}) - depth B

Normal QQ plot of ^{40}K concentrations - depth B

were 11, 14 and 82 Bq kg^{-1}, respectively (Vuković et al. 1996). For CFPP 'Nikola Tesla', Janković et al. (2011) reported mean activity concentrations of ^{238}U, ^{232}Th and ^{40}K in coal of 43, 21 and 120 Bq kg^{-1}; in slag 81, 39 and 241 Bq kg^{-1}; in fly ash 129, 72 and 360 Bq kg^{-1}, respectively. By comparing mean values for radionuclides in both layers obtained here with equivalent data reported for radionuclides around CFPPs worldwide (Table 2), it can be concluded that our results for activity concentrations are similar. The measured activity concentrations of radionuclides in soil at depths A and B were slightly different (Table 1). Charro et al. (2013a) reported similar results, without significant differences for ^{238}U, ^{232}Th and ^{40}K activity concentrations in soil layers at depths from 0 to 30 cm. Dai et al. (2007) found that activity concentrations of ^{226}Ra, ^{232}Th and ^{40}K varied with soil depth from 0 to 50 cm and with distance from CFPP in China. Dragović et al. (2012) showed homogeneous distribution for activity concentrations of natural radionuclides in six different soil types for 0–50-cm profiles.

Deposition consequences of natural radionuclides were estimated using K-parameter calculated as the ratio between the activity concentrations of the radionuclide of interest at two depths. K values significantly higher than 1 indicate a decreasing radionuclide profile. Among the radionuclides, the minimum value of K was 0.7. The maximum value for ^{40}K and ^{238}U was 1.7 and that of ^{232}Th was 2.1. The average value of K for all three radionuclides was 1.0, the same as reported by Charro et al. (2013a).

In order to determine the degree of contamination due to operation of CFPP, the contamination factor (CF) was calculated. This is the ratio obtained by dividing the concentration of each metal in the soil by the baseline or background value (Bhuiyana et al. 2010). Based on their intensity, CFs may be classified on a scale ranging from 1 to 6, where the highest number indicates that the metal concentration is 100 times greater than that expected in the crust (Muller 1969). The background values for topsoil used for ^{238}U, ^{232}Th and ^{40}K were 29.5, 34.05 and 620.2 Bq kg^{-1}, respectively (Salminen et al. 2005). Calculated mean values for CF_s for depths A and B were CF_K—0.9, CF_{Th}—1.5 and CF_U—1.86.

Soil properties such as particle size classes, pH, specific electrical conductivity (SEC), total organic carbon (TOC), carbonate content (CC) and cationic exchange capacity (CEC) may influence migration and adsorption of metals and radionuclides (Dragović et al. 2012). Basic descriptive statistics of the soil properties analysed here are presented in Table 3. The particle size distribution according to the USDA diagram (Baize 1993) shows that the soil texture spread from silt clay loam to sand clay loam. However, most samples belonged to the silty loam or silt textural classes. Soil pH varied from strongly acidic to weakly alkaline (range 4.87–8.16), but most soils were found to be neutral (mean 6.79). SEC ranged from 25.9 to 168 µS cm^{-1}, with a mean value of 77.9 µS cm^{-1}. The TOC content varied from 0.24 to 3.93 % (mean 1.21 %). TOC was suggested to affect the retention and migration of the fallout radionuclides in the environment (Staunton et al. 2002). CC showed significant variations between sampling locations, ranging from 0.05 to 19.7 %. Soil samples with CC higher than 1 % had pH around 8, and SEC was greater than 100 µS cm^{-1}. Carbonate leaching and precipitation, which are influenced by pH, are important factors controlling the solubility of natural radionuclides, especially ^{238}U and ^{232}Th, which become mobile (Winde and van der Walt 2004), can migrate and can be fixed by the organic matter. CEC varied from 15.9 to 99.6–cmol kg^{-1}, with a mean value of 43.1 cmol kg^{-1}.

Table 2 Mean activity concentrations of radionuclides and gamma dose rate based on measurements of soil samples around CFPPs worldwide

Country	Mean activity concentration (Bq kg^{-1})			Gamma dose rate (nGy h^{-1})	Reference
	^{238}U	^{232}Th	^{40}K		
Serbia	50.7	48.6	560	76.3	This study
China	–	49.77	720.57	75.2	Dai et al. (2007)
China	–	59.6	751.2	86.6	Lu et al. (2012)
Turkey	30.5	39.7	378.7	53.9	Aytekin and Baldik (2008)
Hungary	130	25.5	329	89.2	Papp et al. (2002)
Spain	30	43	445	58	Charro et al. (2013b)
Greece	42	36	496	62	Psichoudaki and Papaefthymiou (2008)

– data not reported

Table 3 Descriptive statistics of soil properties for depths A and B and for the average for both depths in soil samples around CFPP 'Nikola Tesla'

| Parameter	Sand (%)			Silt (%)			Clay (%)			pH			SEC (µS cm^{-1})			TOC (%)			CC (%)			CEC (cmol kg^{-1})		
Depth	A	B	Both	A	B	Both	A	B	Both	A	B	Both	A	B	Both	A	B	Both	A	B	Both	A	B	Both
Descriptive statistics																								
Mean	10.0	9.5	9.8	60.9	59.0	59.9	29.1	31.5	30.3	6.8	6.7	6.8	87.6	68.7	78.2	1.4	1.0	1.2	2.6	2.5	2.5	44.6	42.8	43.7
Range	49.2	83.1	65.0	44.4	72.1	57.2	25.3	35.2	27.7	3.1	3.3	3.2	141.1	136.4	121.2	3.4	1.9	2.2	19.6	17.8	18.6	81.3	83.5	81.6
Standard deviation	11.2	13.6	12.2	9.1	11.5	10.4	5.6	6.4	5.6	0.8	0.9	0.9	40.1	35.6	36.4	0.6	0.4	0.4	5.0	4.8	4.9	28.6	29.3	28.9
Minimum	1.9	1.4	1.8	32.6	5.1	19.1	16.0	10.4	14.1	5.0	4.9	4.9	26.9	25.9	26.4	0.5	0.2	0.5	0.1	0.1	0.1	18.2	15.9	17.9
Maximum	51.1	84.0	66.8	77.0	77.1	76.3	41.4	45.6	41.7	8.1	8.2	8.1	167.9	162.3	147.6	3.9	2.1	2.7	19.7	17.9	18.7	99.6	99.4	99.5

Assessment of the radiological hazards

The external dose rate and hazard index of γ-ray radiation were estimated using average values for activity concentrations of ^{238}U, ^{232}Th and ^{40}K for both soil depths A and B, since the dose rate above the ground at 1 m arises from radionuclides deposited on the upper surface of the soil (UNSCEAR 2000). Descriptive statistics for total absorbed dose rate, annual effective dose rate, external hazard index and excess lifetime cancer risk outdoors for all 72 sampling locations are presented in Table 1.

The spatial distribution of total absorbed gamma dose rates (D) arising from members of terrestrial radionuclides from the uranium and thorium decay chains and from ^{40}K in the soils around the CFPP is presented in Fig. 3. Total gamma dose rates varied between 41.9 and 93.0 nGy h^{-1} (mean 76.3 nGy h^{-1}). Under normal circumstances, the total dose rate from terrestrial radionuclides is 60 nGy h^{-1} (UNSCEAR 2000). A mean value of 60.5 nGy h^{-1} was reported for Belgrade (Janković-Mandić and Dragović 2010). While bearing in mind that the soil was the same type as that in this study, the higher value for mean D could be attributed to pollution at some sampling locations. In other parts of Serbia, mean values for D_s were 78.8 (Bikit et al. 2005) and 66.8 nGy h^{-1} (Dragović et al. 2006). When comparing these findings, one should have in mind that the study of Bikit et al. (2005) comprised 50 samples from Vojvodina, while Dragović et al. (2006) examined a total of 140 samples from 21 regions in Serbia and Montenegro. The regions investigated in these studies differ with respect to age, genesis, mineral content and petrochemical and geochemical characteristics. The total absorbed gamma dose rates around CFPPs worldwide are presented in Table 2.

To estimate the annual effective dose using Eq. 2, the conversion coefficient and outdoor occupancy factor from the absorbed dose in air must be considered. In this study, estimated annual effective dose values ranged from 51.4 to 114.15 µSv. Estimated values were about 10 times lower than the maximum permissible dose of 1 mSv recommended by the ICRP for members of the public (ICRP 2007). According to UNSCEAR (2000), the worldwide average for annual effective dose, estimated on the basis of primordial radiation sources of terrestrial origin, is 70 µSv. The mean value of estimated annual effective dose around the CFPP complex was 93.6 µSv, which is almost one order of magnitude higher than the world average.

The value of the external hazard index must be lower than unity in order to keep the radiation hazard

Fig. 3 The spatial distribution of total absorbed gamma dose rates arising from members of terrestrial radionuclides from the uranium and thorium decay chains and from ^{40}K in the soils of the study area
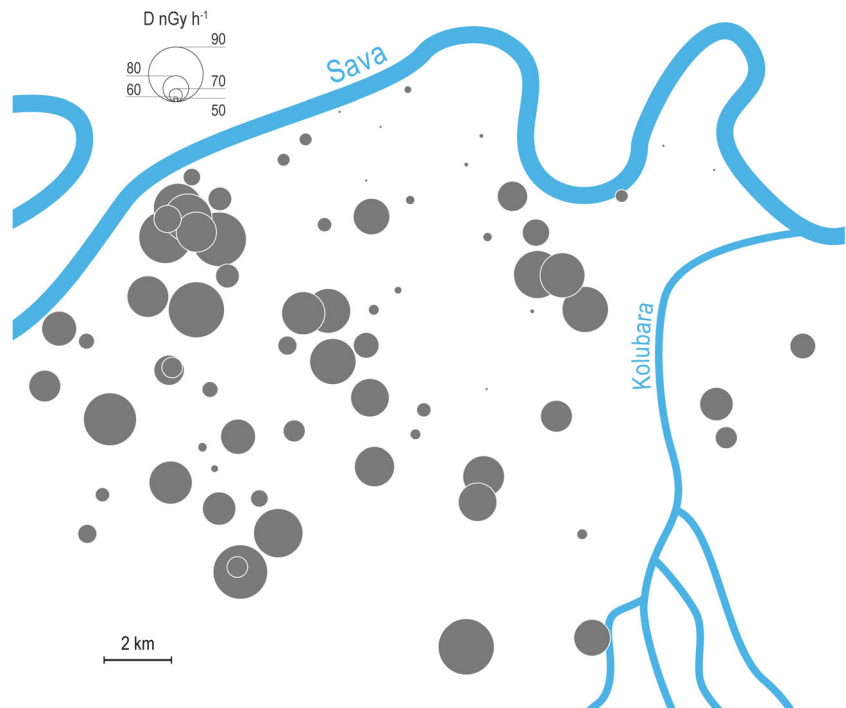
insignificant. Descriptive statistics for H_{ex} calculated according to Eq. 3 are presented in Table 1. The maximum value was 0.54, which indicates that soil from the study area is of no significant radiological threat to the population.

The mean excess lifetime cancer risk for all sample locations is 3.6×10^{-4}, which is less than the world average of 2.9×10^{-3} (UNSCEAR 2000). This implies that the chance of developing cancer, due to work at the power plant, by people living around it is generally insignificant. In comparison with data reported by Janković-Mandić and Dragović (2010) for the territory of Belgrade, Serbia, the mean value for ELCR found here is slightly higher.

Cluster analysis

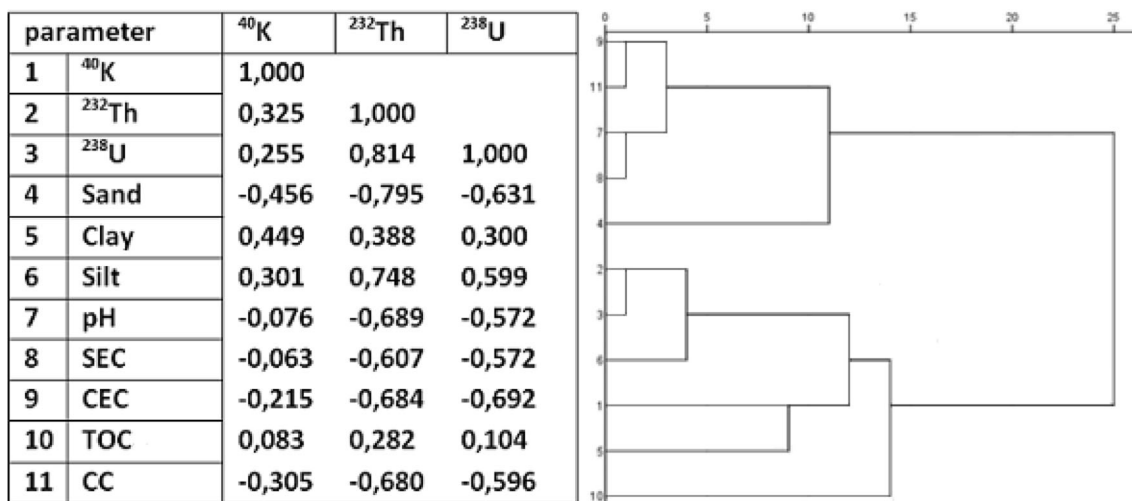The agglomeration schedule of CA based on a between-groups linkage method and Pearson

parameter		^{40}K	^{232}Th	^{238}U
1	^{40}K	1,000		
2	^{232}Th	0,325	1,000	
3	^{238}U	0,255	0,814	1,000
4	Sand	-0,456	-0,795	-0,631
5	Clay	0,449	0,388	0,300
6	Silt	0,301	0,748	0,599
7	pH	-0,076	-0,689	-0,572
8	SEC	-0,063	-0,607	-0,572
9	CEC	-0,215	-0,684	-0,692
10	TOC	0,083	0,282	0,104
11	CC	-0,305	-0,680	-0,596

Fig. 4 Pearson correlation coefficients and dendrogram derived from the cluster analysis of radionuclide activity concentrations and soil properties

correlation as an amalgamation rule was applied in order to examine the correlation between activity concentrations of the investigated radionuclides and soil properties. The results obtained are presented in a dendrogram together with the derived Pearson product moment correlation coefficient (Fig. 4). Two main clusters can be observed: the first comprising CEC, CC, pH, SEC and sand and the second consisting of ^{232}Th, ^{238}U, clay, ^{40}K, slit and TOC. Navas et al. (2011) reported that the relatively weak correlations of ^{238}U with the other radionuclides might be due to its relatively high mobility, which was detected in the

soil depth profiles. The highest Pearson correlation coefficient was derived for ^{238}U with ^{232}Th, which indicates a common source. It is well documented that radionuclides are adsorbed onto clay surfaces or fixed within the lattice structure (Jasinka et al. 1982; VandenBygaart and Protz 1995). In this study, all radionuclides were positively correlated with clay and silt fractions but showed negative correlations with sand. This correlation analysis confirmed results obtained worldwide showing that the fine-grained soil fraction has a higher tendency for radionuclide adsorption than coarse-grained soils because the soil particle
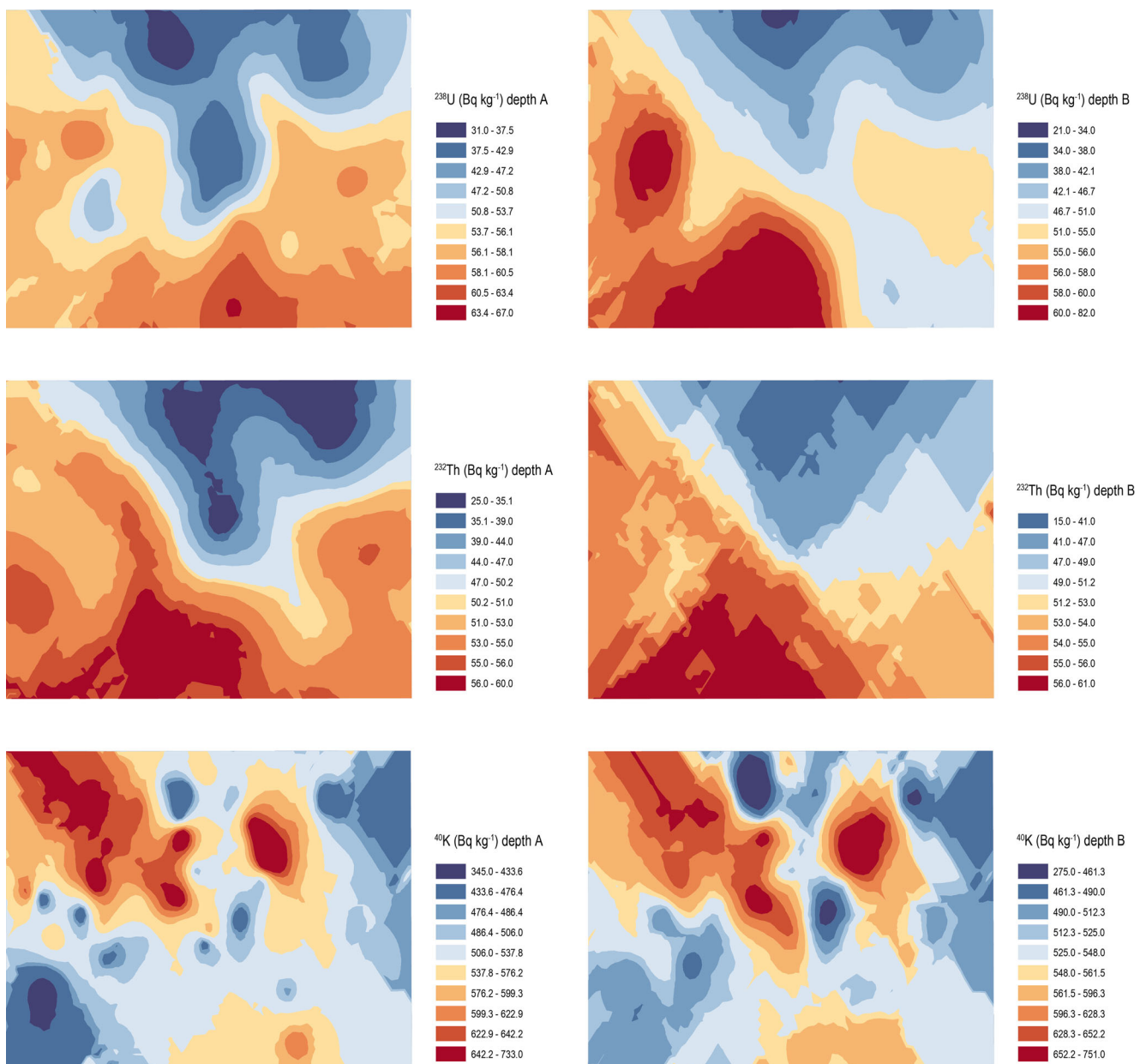

Fig. 5 The spatial distribution of ^{238}U, ^{232}Th and ^{40}K concentrations in soil from the study area obtained by ordinary kriging

surface area is larger (Baeza et al. 1995; Dragović et al. 2012; Navas et al. 2002). Negative correlations between pH and radionuclides were found, which agrees with the findings of Navas et al. (2002) and Tsai et al. (2011). Specific electrical conductivity and cationic exchange capacity show negative correlations with radionuclide activity concentrations. Organic matter is a component of great importance because it tends to form soluble or insoluble complexes with radionuclides, which can migrate throughout the profile or be retained in the soil (Campbell 1978; Vega et al. 2004). Positive but not significant correlation was found between the total organic carbon content and radionuclide activity concentrations, which confirms earlier results (Dragović et al. 2012; Ligero et al. 2001; Navas et al. 2002). Organic matter contains functional groups that can form complexes with radionuclides. This complexation affects radionuclide mobility, adsorption to soils and bioavailability (Koch-Steindl and Pröhl 2001). The strong negative correlation of radionuclides, ^{238}U and ^{232}Th, with carbonate content suggests binding to soil minerals other than calcite, probably to silicates derived during weathering processes from parent rocks.

Geostatistical analysis

The spatial distribution of uranium, thorium and potassium concentrations in soil from the territory around the CFPP obtained by ordinary kriging is presented in Fig. 5. After visual inspection of semivariograms and cross-validation, the best fit model in depth A for the prediction of ^{238}U and ^{40}K was exponential, but for ^{232}Th, it was Gaussian. The best fit model in depth B for the prediction of ^{238}U was Gaussian and for ^{232}Th exponential, and for ^{40}K, it was circular. Semivariogram models of ^{238}U, ^{232}Th and ^{40}K and their parameters are shown in Table 4. The corresponding nugget, sill and range values, as well as nugget/sill ratio, of the best fitted theoretical models are presented in Table 5. The nugget/sill ratio of variance expressed as a percentage can be a criterion for classifying the spatial dependence of radionuclide concentrations. If the nugget/sill ratio is less than 25 %, then the variable has strong spatial dependence; if the ratio is between 25 and 75 %, the variable has moderate spatial dependence, and if the ratio is greater than 75 %, the variable shows weak spatial dependence (Xie et al. 2007). Based on the nugget/sill ratio value, it can be concluded that the variable has moderate spatial dependence for ^{238}U at depths A and B and for ^{232}Th at depth A, with ratio values of 30.6, 56.1 and 27.9 %, respectively. The ratio of ^{232}Th at depth B is 90.1 showing weak spatial dependence. The nugget/sill ratios of ^{40}K at depths A

Table 4 Values of model parameters used to find the best semivariogram

Depth	Model	Radionuclide														
		^{238}U					^{232}Th					^{40}K				
		ME	RMSE	ASE	MSE	RMSSE	ME	RMSE	ASE	MSE	RMSSE	ME	RMSE	ASE	MSE	RMSSE
A	Circular	−0.2398	8.3523	10.8253	−0.0147	0.8808	−1.4147	6.1555	12.5598	−0.0626	0.9245	0.9712	76.3067	76.9310	0.0096	0.9917
	Spherical	−0.2511	8.3453	10.8234	−0.0154	0.8810	−1.4176	6.1517	12.5584	−0.0598	0.9324	1.0335	76.2736	76.5644	0.0105	0.9958
	Exponential	**−0.2587**	**8.3142**	**10.4018**	**−0.0153**	**0.9249**	−1.5618	6.2164	13.3123	−0.0549	0.9107	**0.2476**	**75.2338**	**74.9522**	**0.0053**	**1.0081**
	Gaussian	−0.2336	8.3635	10.7511	−0.0162	0.8846	**−1.4256**	**6.1914**	**12.3188**	**−0.0307**	**1.0173**	0.9819	76.7444	77.8428	0.0089	0.9866
B	Circular	0.1091	10.8500	10.9602	0.0075	0.9995	−36.0288	89.1587	279.8222	−0.0634	0.3275	**1.4484**	**74.3491**	**73.6310**	**0.0174**	**1.0150**
	Spherical	0.1033	10.8478	10.9665	0.0076	1.0003	−35.8287	88.8249	278.9063	−0.0610	0.3263	1.0155	74.2697	72.2128	0.0191	1.0510
	Exponential	0.1636	10.9141	10.9179	0.0127	1.0098	**−35.7404**	**88.6688**	**278.3295**	**−0.0583**	**0.3286**	1.6025	73.3750	71.7391	0.0202	1.0318
	Gaussian	**0.0607**	**10.8309**	**10.9656**	**0.0040**	**0.9996**	−36.1875	89.4866	280.5790	−0.0607	0.3289	2.1176	74.4392	74.3638	0.0270	1.0172

Bold values were used for prediction of ^{238}U, ^{232}Th and ^{40}K

Table 5 Best-fitted semivariogram models of radionuclides and their parameters for depths A and B

Depth	Radionuclide					
	^{238}U		^{232}Th		^{40}K	
	A	B	A	B	A	B
Model	Exponential	Gaussian	Gaussian	Exponential	Exponential	Circular
Nugget	4.8×10^8	2.1×10^3	1.1×10^{12}	2.6×10^{16}	0	2.2×10^5
Sill	1.6×10^9	3.8×10^3	3.8×10^{12}	2.9×10^{16}	7.7×10^3	1.1×10^6
Range (km)	12.2	9.5	8.9	1.6	4.4	3.3
Nugget/Sill	0.31	0.56	0.28	0.90	0	0.21

and B are 0 and 20.7 %, respectively, suggesting that the variables have strong spatial dependence.

The ranges for ^{238}U, ^{232}Th and ^{40}K at depth A are 12.2, 8.9 and 4.4 km and at depth B are 9.5, 1.6 and 3.3 km, respectively. This shows that the length of the spatial autocorrelation is longer than the average sampling interval of 1.15 km, which indicates that the sampling design is appropriate, so it is expected that spatial structures on the interpolated map will be good.

From Fig. 5, it is clear that the concentrations of ^{238}U, ^{232}Th, and ^{40}K varied with distance from the CFPP and soil depths. The highest activity concentrations of ^{238}U and ^{232}Th were in the south and west of the power plant, which could be attributed to the dominant wind direction. These results are in accordance with dispersion models of fly ash emissions reported by Milutinović et al. (2012). Distribution patterns of ^{40}K did not show elevated concentrations in this direction, already in the area with planosol pedology. The spatial distribution patterns of ^{226}Ra, ^{232}Th, ^{210}Pb, ^{210}Po and ^{40}K in the soil, as well as their ratios, did not indicate any significant perturbation of their natural concentrations in the soil of Bavaria (Bunzl et al. 1984). The prediction maps of Dai et al. (2007) evaluated activity concentrations of radionuclides in the vicinity of a CFPP in China. Decreases with distance away from the CFPP and geographical trends were revealed, with high concentrations in the NW–SE direction caused by the prevailing wind. Charro et al. (2013b) pointed out that radionuclides followed two different models of spatial distribution around a CFPP in Spain. The first group (^{238}U, ^{226}Ra, ^{232}Th, ^{224}Ra and ^{40}K) was assigned as 'natural background radioactivity', and the second (^{210}Pb and ^{137}Cs) was labelled as 'atmospheric fallout radioactivity'. Neither of these two groups followed a spatial trend, suggesting that the CFPP was the source of the measured radionuclides.

Conclusion

The activity concentrations of ^{238}U, ^{232}Th and ^{40}K in soil samples collected in the area surrounding the coal-fired power plant were determined by gamma-ray spectrometry. The activity concentrations of primordial radionuclides varied from 21 to 82 Bq kg^{-1} for ^{238}U, from 15 to 61 Bq kg^{-1} for ^{232}Th and from 275 to 751 Bq kg^{-1} for ^{40}K. The mean value of the estimated annual effective dose due to these radionuclides was 93.6 μSv. Applying cluster analysis, correlations between radionuclide activity concentrations and soil properties were investigated. Two clusters were derived: the first comprised CEC, CC, pH, SEC and sand and the second consisted of ^{232}Th, ^{238}U, clay, ^{40}K, silt and TOC. The highest Pearson correlation coefficient was obtained for ^{238}U with ^{232}Th indicating a common source. A geostatistical mapping tool based on kriging was used to build maps of the radionuclide activity concentrations and total absorbed dose rate. The maps of radionuclide distribution revealed areas with the highest activity concentrations of ^{238}U and ^{232}Th in the south and the west of the plants, in the dominant wind direction, which is in accordance with dispersion models of fly ash emissions. The results obtained here can be used as a valuable database for future estimations of the impact of radioactive pollution around the CFPP and for the developmental prospects of the region. They will also be of significance for the instigation of studies on environmental protection during the construction of the planned new block of the coal-fired power energy industry in Serbia.

References

ASTM (American Society for Testing and Materials) (1983) Standard method for sampling surface soil for radionuclides - method C 998-83. vol. 11.03. ASTM, Philadelphia

ASTM (American Society for Testing and Materials) (1988) Construction: cement, lime, gypsum, vol. 04.01. ASTM, Philadelphia

Aytekin H, Baldik R (2008) On the radiological character of a coal-fired power plant at the town of Çatalağzi, Turkey. Turkish J Eng Env Sci 32:101–105

Baeza A, Del Rio M, Jimenez A, Miro C, Paniagua J (1995) Influence of geology and soil particle size on the surface-area/volume activity ratio for natural radionuclides. J Radioanal Nucl Chem 189:289–299

Baize D (1993) Soil science analyses: a guide to current use. Wiley, Chichester

Beretka J, Mathew PJ (1985) Natural radioactivity of Australian building materials, industrial wastes and by-products. Health Phys 48:87–95

Bhuiyana MAH, Parvezb L, Islamc MA, Dampared SB, Suzukia S (2010) Heavy metal pollution of coal mine-affected agricultural soils in the northern part of Bangladesh. J Hazard Mater 173:384–392

Bikit I, Slivka J, Lj Č, Krmar M, Vesković M, Žikić-Todorović N et al (2005) Radioactivity of the soil in Vojvodina (northern province of Serbia and Montenegro). J Environ Radioact 78:11–19

Brereton RG (2003) Data analysis for the laboratory and chemical plant. Wiley, West Sussex

Bunzl K, Hotzl H, Rosner G, Winkler R (1984) Spatial distribution of radionuclides in soil around a coal-fired power plant: ^{210}Pb, ^{210}Po, ^{226}Ra, ^{232}Th, ^{40}K emitted with the fly ash and ^{137}Cs from the worldwide weapon testing fallout. Sci Total Environ 38:15–31

Campbell CA (1978) Developments in soil science. In: Schnitzer M, Khan SV (eds) Soil organic matter. Elsevier, Amsterdam, pp 173–265

Charro E, Pardo R, Peña V (2013a) Chemometric interpretation of vertical profiles of radionuclides in soil near a Spanish coal-fired power plant. Chemosphere 90:488–496

Charro E, Pardo R, Peña V (2013b) Statistical analysis of the spatial distribution of radionuclides in soils around a coal-fired power plant in Spain. J Environ Radioact 124:84–92

Clarke LB, Sloss LL (1992) Trace elements, emissions from coal combustion and gasification. IEA Coal Research, IEA CR/49. London

Dai L, Wei H, Wang L (2007) Spatial distribution and risk assessment of radionuclides in soils around a coal-fired power plant: a case study from the city of Baoji, China. Environ Res 104:201–208

Dragović S, Onjia A (2006) Classification of soil samples according to their geographic origin using gamma-ray spectrometry and principal component analysis. J Environ Radioact 89:150–158

Dragović S, Jankovic L, Onjia A (2006) Assessment of gamma dose rates from terrestrial exposure in Serbia and Montenegro. Radiat Prot Dosim 121:297–302

Dragović S, Gajić B, Dragović R, Janković-Mandić L, Slavković-Beškoski L, Mihailović N, Momčilović M, Ćujić M (2012) Edaphic factors affecting the vertical distribution of radionuclides in the different soil types of Belgrade, Serbia. J Environ Monit 14:127–137

ESRI (2009) ArcGIS desktop: release 9.3. Environmental Systems Research Institute, Redlands

Federal Geological Survey (1980) Geological Map of the Socialist Federal Republic of Yugoslavia 1:100000, sheet Obrenovac, Belgrade

Gokalp Z, Basaran M, Uzun O, Serin Y (2010) Spatial analysis of some physical soil properties in a saline and alkaline grassland soil of Kayseri, Turkey. Afr J Agric Res 5:1127–1137

IAEA (International Atomic Energy Agency) (2004) Soil sampling for environmental contaminants. IAEA-TECDOC-1415, Vienna

ICRP (International Commission on Radiological Protection) (2007) The 2007 Recommendations of the International Commission on Radiological Protection. ICRP Publication 103. Ann. ICRP 37. Pergamon, Oxford

Ilic M, Cheeseman C, Sollares C, Knihgt J (2003) Mineralogy and microstructure of sintered lignite coal fly ash. Fuel 82:331–336

Institute of Soil Science (1963) Pedological Map of the Socialist Federal Republic of Yugoslavia 1:50000, Belgrade

ISO 10390 (2005) Soil quality – determination of ph. International Standard Organization, Geneva

ISO 10693 (1995) Soil quality – determination of carbonate content – volumetric method. International Standard Organization, Geneva

ISO 11265 (1994) Soil quality – determination of the specific electrical conductivity, International Standard Organization, Geneva

Janković MM, Todorović DJ, Nikolić JD (2011) Analysis of natural radionuclides in coal, slag and ash in coal-fired power plants in Serbia. J Min Metall Sect B-Metall 47:149–155

Janković-Mandić L, Dragović S (2010) Assessment of terrestrial gamma exposure to the population of Belgrade (Serbia). Radiat Prot Dosim 140:369–377

Janković-Mandić L, Dragović R, Dragović S (2010) Distribution of lithogenic radionuclides in soils of the Belgrade region (Serbia). J Geochem Explor 105:43–49

Jasinka M, Niewiadomski T, Schwbenthan J (1982) In: Vohra K, Mishra UC, Pillai KC, Sadasivan S (eds) Natural radiation environment. Wiley, New York, pp 206–211

Koch-Steindl H, Pröhl G (2001) Considerations on the behavior of long-lived radionuclides in the soil. Radiat Environ Biophys 40:93–104

Külahci F, Şen Z (2008) Multivariate statistical analyses of artificial radionuclides and heavy metals contaminations in deep mud of Keban Dam Lake, Turkey. Appl Radiat Isotopes 66:236–246

Ligero RA, Ramos-Lerate I, Barrera M, Casas-Ruiz M (2001) Relationships between sea-bed radionuclide activities and some sedimentological variables. J Environ Radioact 57:7–19

Lu X, Li X, Yun P, Luo D, Wang L, Ren C, Chen C (2012) Measurement of natural radioactivity and assessment of associated hazards in soil around Baoji second coal-fired thermal power plant, China. Radiat Prot Dosim 148:219–226

Matheron G (1963) Principles of geostatistics. Econ Geol 58:1246–1266

Matheron G (1965) Les variables régionalisées et leur estimation: une application de la théorie des fonctions aléatoires aux sciences de la nature. Masson, Paris

Milutinović P, Gršić Z, Živković N, Dramlić D, Velikić Z, Dramlić S (2012) System for automatically preventing the raising of ash from dedicated landfills. Chem Ind Chem Eng Q 18:681–692

Muller G (1969) Index of geoaccumulation in sediments of the Rhine River. Geo J 2:108–118

Navas A, Soto J, Machín J (2002) ^{238}U, ^{226}Ra, ^{210}Pb, ^{232}Th and ^{40}K activities in soil profiles of the flysch sector (Central Spanish Pyrenees). Appl Radiat Isot 57:579–589

Navas A, Valero-Garcés B, Gaspar L, Palazón L (2011) Radionuclides and stable elements in the sediments of the Yesa Reservoir, Central Spanish Pyrenees. J Soils Sediments 11:1082–1098

ORTEC (2001) Gamma vision 32, gamma-ray spectrum analysis and mca emulation, Version 5.3. ORTEC, Oak Ridge, USA

Papastefanou C (2010) Escaping radioactivity from coal-fired power plants (CPPs) due to coal burning and the associated hazards: a review. J Environ Radioact 101:191–200

Papp Z, Dezső Z, Daróczy S (2002) Significant radioactive contamination of soil around a coal-fired thermal power plant. J Environ Radioact 59:191–205

Parmaksiz A, Arikan P, Vural M, Yeltepe E, Tükenmez I (2011) [226]Ra, [232]Th and [40]K radionuclides enhancement rate and dose assessment for residues of lignite-fired thermal power plants in Turkey. Radiat Prot Dosim 147:548–554

Psichoudaki M, Papaefthymiou H (2008) Natural radioactivity measurements in the city of Ptolemais (Northern Greece). J Environ Radioact 99:1011–1017

Rowell DL (1997) Bodenkunde. Untersuchungsmethoden und ihre Anwendungen. Springer, Berlin

Salminen R, Batista MJ, Bidovec M, Demetriades A, De Vivo B, De Vos W et al. (2005) Geochemical atlas of Europe. Part 1. Background information, methodology and maps, Geological Survey of Finland, Espoo

Simakov VN (1957) Application of phenylanthranilic acid in determining humus, the method of Tyurin. Почвоведение 8:72–73

Soil Conservation Service (1972) Soil survey laboratory. Methods and procedures for collecting soil samples. Soil survey report 1. U.S.D.A., Dept. Agric., WA, USA

SPSS (Statistical Package for the Social Sciences) (2007) V. 16.0. SPSS, Chicago, Illinois

Staunton S, Dumat C, Zsolnay A (2002) Possible role of organic matter in radiocaesium adsorption in soils. J Environ Radioact 58:163–173

Tsai T, Liu C, Chuang C, Wei H, Men L (2011) The effects of physico-chemical properties on natural radioactivity levels, associated dose rate and evaluation of radiation hazard in the soil of Taiwan using statistical analysis. J Radioanal Nucl Chem 288:927–936

Tsikritzis LI (2005) Chemometrics of the distribution and origin of [226]Ra, [228]Ra, [40]K and ^{137}Cs in plants near the West Macedonia Lignite Center (Greece). J Radioanal Nucl Chem 264:651–656

UNCSEAR (United Nations Scientific Committee on the Effects of Atomic Radiation) (2010) Report to the general assembly with scientific annexes. Annex B: exposure of the public and workers from various sources of radiation. United Nations, New York

UNSCEAR (United Nations Scientific Committee on the Effects of Atomic Radiation) (2000) Sources and effects of ionizing radiation. Report to general assembly, with scientific annexes. United Nations, New York

VandenBygaart AJ, Protz R (1995) Gamma radioactivity on a chronosequence, Pinery Provincial Park, Ontario. Can J Soil Sci 75:73–84

Vega FA, Covelo EF, Andrade ML, Marcet P (2004) Relationship between heavy metals content and soil properties in minesoils. Anal Chim Acta 524:141–150

Vuković Ž, Mandić M, Vuković D (1996) Natural radioactivity of ground waters and soils in the vicinity of the ash repository of the coal-fired power plant Nikola Tesla A – Obrenovac (Yugoslavia). J Environ Radioact 33:41–48

Walkley A, Black IA (1934) An examination of the Degtjareff method for determining soil organic matter and a proposed modification of the chromic acid titration method. Soil Sci 37:29–38

Winde F, van der Walt IJ (2004) The significance of groundwater–stream interactions and fluctuating stream chemistry on waterborne uranium contamination of streams—a case study from a gold mining site in South Africa. J Hydro 287:178–196

Xie Z, Li J, Wu W (2007) Application of GIS and Geostatistics to Characterize Spatial Variation of Soil Fluoride on Hang-Jia-Hu Plain, China. Int Fed Info Proc 258:253–266

Životić D, Gržetić I, Lorenz H, Simić V (2008) U and Th in some brown coals of Serbia and Montenegro and their environmental impact. Environ Sci Pollut R15:155–161